



“Comet-tail” ejecta streaks: A predicted cratering landform unique to Titan

Ralph D. LORENZ

Lunar and Planetary Laboratory, University of Arizona, 1629 E. University Boulevard, Tucson, Arizona 85721, USA
E-mail: rlorenz@lpl.arizona.edu

(Received 22 August 2003; revision accepted 10 February 2004)

Abstract—A model for an impact ejecta landform peculiar to Saturn’s moon Titan is presented. Expansion of the ejecta plume from moderate-sized craters is constrained by Titan’s thick atmosphere. Much of the plume is collimated along the incoming bolide’s trajectory, as was observed for plumes from impacts on Jupiter of P/Shoemaker-Levy-9, but is retained as a linear, diagonal ejecta cloud, unlike on Venus where the plume “blows out.” On Titan, the blowout is suppressed because the vertically-extended atmosphere requires a long wake to reach the vacuum of space, and the modest impact velocities mean plume expansion along the wake is slow enough to allow the wake to close off. Beyond the immediate ejecta blanket around the crater, distal ejecta is released into the atmosphere from an oblique line source: this material is winnowed by the zonal wind field to form streaks, with coarse radar-bright particles transported less far than fine radar-dark material. Thus, the ejecta form two distinct streaks faintly reminiscent of dual comet tails, a sharply W-E radar-dark one, and a less swept and sometimes comma-shaped radar-bright one.

INTRODUCTION

Titan, with a radius of 2575 km, is the largest satellite of Saturn and the second-largest satellite in the solar system. Titan has the remarkable distinction of being the only satellite with a significant atmosphere (e.g., Lorenz and Mitton 2002), one which has so far prevented studies of its impact crater population. Despite its small size, Titan has a predominantly nitrogen atmosphere with a surface pressure of 1.5 bar and a temperature of 94 K. In Titan’s low gravity, the atmosphere is vertically very extended, with a scale height 3–8 times larger than that of Earth. The column mass of gas is around 10 times higher than on Earth and the surface density is 4 times higher than that of Earth’s atmosphere.

Many aspects of Titan’s atmosphere and surface-atmosphere interactions will be explored by the NASA-ESA Cassini-Huygens mission, which will arrive at Saturn in the summer of 2004 and study Titan for 4 years from orbit with a wide array of instruments. Titan’s surface, and its as-yet-unknown but probably extensive impact crater population (Lorenz 1997), will be studied by a near-infrared spectrometer and an imaging radar (which is unaffected by the organic haze in Titan’s atmosphere) and by optical imaging. Additionally, in early 2005, the parachute-borne Huygens probe will make a 2.5 hr descent through the atmosphere making in situ investigations.

Here I show how the combination of Titan’s west-east

zonal winds and its extreme vertical extent may control the distribution of distal impact ejecta to form downwind fallout blankets that have distinct light and dark (in radar) streaks. This geometry may be peculiar to Titan and may provide insight into the impact plume expansion process. Contrasting the distal ejecta distribution around Titan craters with those observed on Venus will be particularly illuminating where distinctive parabolae were observed.

DISPERSAL OF FINE EJECTA IN LARGE IMPACTS

In an impact event, most of the material removed from the crater is deposited in the immediate vicinity of it as a contiguous ejecta blanket. However, a small component may be dispersed more widely, but exactly how depends on the details of the interaction of the impact fireball with the atmosphere (e.g., Melosh 1989)—this interaction is summarized in Fig. 1.

The hot cloud of vapor created by the impact event can be assumed to expand to a pressure equivalent to the surface atmospheric pressure on the planet—this cloud has a radius (R). If this radius is large in comparison to the atmospheric scale height (H), then the cloud feels less pressure on top and can continue to expand upward. In such a situation, which requires large (>10 km-diameter crater) cratering events, the vapor cloud continues to expand upward and outward, launching entrained material and rock droplets that condense

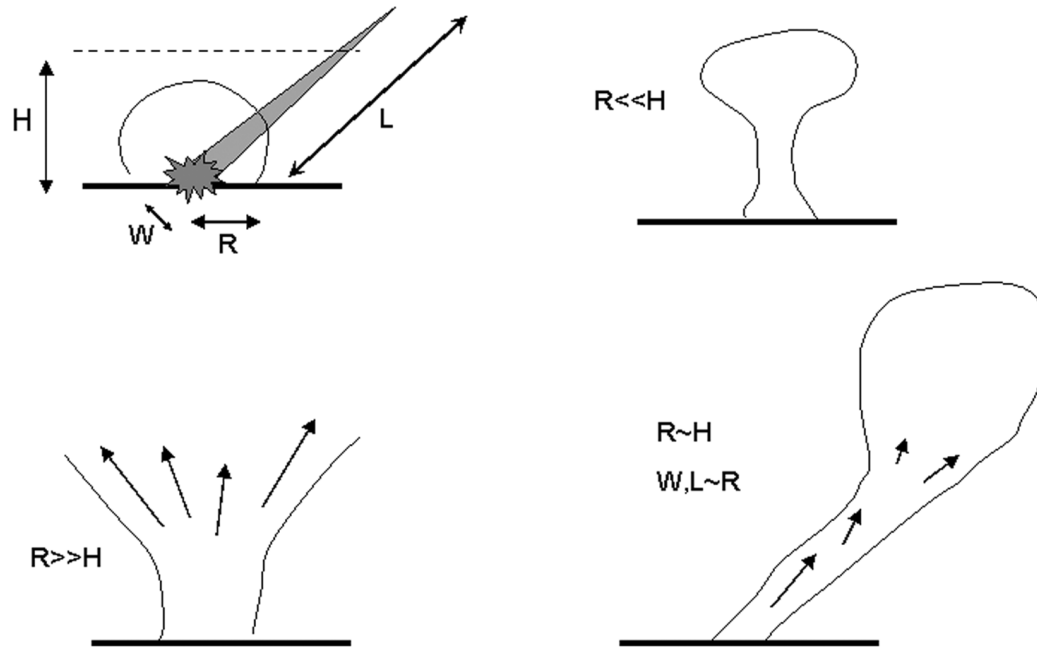


Fig. 1. Schematic of the interaction of the impact fireball with the atmosphere and bolide vacuum tunnel. R is the radius of the equilibrated fireball (i.e., a measure of impact energy), H is the scale height of the atmosphere, L is the length of the “vacuum tunnel” caused by the bolide, between the surface and the point where it has closed again, and W is the diameter of the tunnel, assumed to be the same as the diameter of the crater. Upper right shows mushroom cloud typical of small impacts and explosions, leading to simple downwind streaks. Lower left shows explosive expansion to give wide dispersal of ejecta as in Venusian parabolae and terrestrial microtektites. Lower right shows collimated expansion characteristic of SL-9 impacts and probably many of Titan’s features.

from the vapor onto high-speed ballistic trajectories above the atmosphere. This process leads to the wide dispersal of microtektites. Among the terrestrial craters where this is known to have occurred are the Ries, Bosumtwi, Chesapeake, and the unknown source crater of the Australasian microtektite field. Recently, a microtektite deposit was discovered in England that is believed to be associated with the Manicouagan impact structure in Canada (Walkden et al. 2002).

When the crater is of low energy, $R < H$ and expansion stops. The approximately spherical cloud will still be very hot, and thus buoyant, and will rise to form the familiar mushroom cloud of large explosions. Any condensing rock vapor, or entrained particulates, will eventually fall out in a simple streak downwind of the crater.

However, there is another aspect to the process which was strikingly observed in the impacts of comet Shoemaker-Levy-9 (SL-9) into Jupiter in 1994. The fireball expansion was noted to be somewhat collimated along the incoming trajectory of the projectile. In essence, the passage of the projectile at hypersonic speeds creates a partial vacuum behind it (or at least a hot, rarified region). The fireball expands preferentially along this vacuum tunnel. This effect has been observed in laboratory tests of impact under an atmosphere (e.g., Shultz 1992; Fig. 13b) and is very well reproduced in models of the SL-9 impacts (e.g., Crawford 1996.) Eventually, the fireball expanding along the tunnel will either feel lower pressure

above it and expand upward, or it will meet the end of the tunnel and will be trapped within the atmosphere.

Reconstruction of the trajectories of the ejecta clouds from SL-9 impacts A and G as observed by the Hubble Space Telescope (Jessup et al. 2000) indicate that their ballistic trajectories had launch angles of $60\text{--}80^\circ$ compared with the 45° inclination of the impactors. Thus, in this case, the fireballs were substantially ducted along the tunnel and then expanded upward and outward (also see Zahnle [1996]). However, note that in this event, attention has been focused on the luminous ejecta observable from Earth, and on the very fine suspended material that remained visible suspended in the jovian atmosphere long afterward. A substantial amount of coarser material was undoubtedly never observed, but quickly fell into Jupiter’s inaccessible depths. This material is responsible for much of the observable surface ejecta on other planets.

VENUSIAN PARABOLAE AND TITAN PREDICTION

Large, radar-dark parabolic features were observed around many recent impact craters on Venus (e.g., Campbell et al. 1992). Vervack and Melosh (1992) found that the parabolic features could be reproduced by a model of ejecta deposited on top of the atmosphere in a circle around the source crater, with a mean particle size falling off with

distance from the impact. As the ejecta fell back through the atmosphere at terminal velocity to the venusian surface, it was winnowed by the zonal (E-W) winds. Since small ejecta falls slower, its horizontal displacement by wind from the initial wider circles is larger and, thus, E-W parabolae are formed by the superposition of displaced rings. Schaller and Melosh (1998) made a detailed study, fitting this model to all the known parabolic features.

Figure 2 shows a prime example of such a feature around the crater Adivar (31 km across). Not only is there a prominent radar-dark parabola (darker than the surrounding terrain, not shown), but the area within the dark parabola is brighter than the surrounding area. At the incidence angles used in synthetic aperture radar mapping, dark probably means terrain smooth on wavelength scales, and thus, mantled with particles smaller than the wavelength, while the bright area denotes an area roughened by the deposition of boulders larger than the wavelength. A “jet” feature can also be seen, flaring west of the crater and expanding—this may be a signature of ejecta caught in the vacuum tunnel that has not exploded out into space.

On Venus, the temperature (and scale height) fall rapidly with altitude, so the atmosphere becomes significant only at an altitude below 150 km or so. One peculiarity of Titan is the large scale height, primarily due to its low gravity. In addition, a sharp increase of temperature with altitude occurs between about 40 and 80 km due to sunlight absorption by the photochemical haze. This increase in temperature causes an increase in scale height (from about 20 to about 40 km) above the first two scale heights, and the altitude at which a given isobar (or more relevantly, density contour) is encountered is (except for the lowest altitudes) much higher on Titan than on Venus, as shown in Fig. 3.

Ejecta particles of 1 mm to 10 cm traverse their own mass of atmosphere over ~ 100 km distances (i.e., become appreciably affected by drag on the landform length scales under discussion in this paper) when the atmospheric density is 10^{-5} to 10^{-3} kg m $^{-3}$. Thus, ballistic or near-ballistic trajectories can occur on Earth and Venus above altitudes of ~ 40 –110 km, but on Titan, they do not occur until altitudes of 200–500 km—a greater height than the horizontal length scale of ejecta features considered here. (The martian atmosphere has a density of only 10^{-2} kg m $^{-3}$ even at the surface and, thus, has only very local effects on plume expansion and is not considered further here.)

The impact plume will expand with a velocity of around half the impact velocity (Melosh and Vickery 1991.) To reach altitudes where the ejecta can be transported ballistically, it takes ~ 2 –5 sec on Earth and Venus where impact velocities of 20–30 km/s are typical. The speeds of sound in the venusian and terrestrial atmospheres are 200–400 m/s in the relevant altitude range (the speed of sound in the planetary atmospheres considered here does not vary strongly due to the square root dependence on temperature divided by molecular mass (see Lorenz and Hubbard [2001] for a

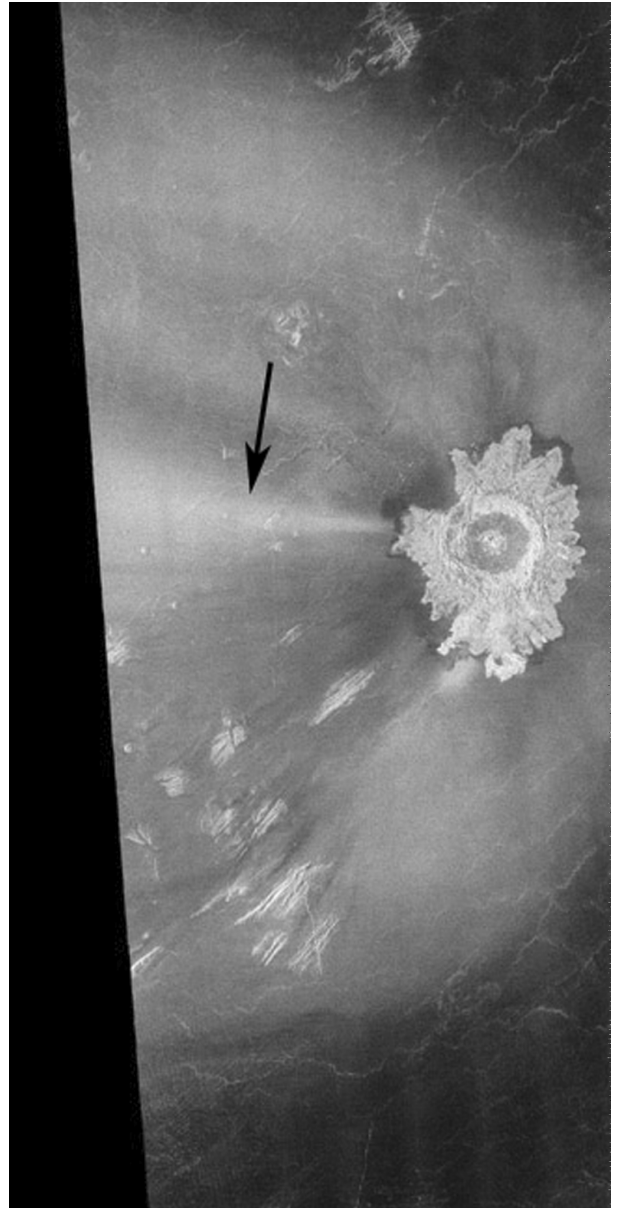


Fig. 2. Parabola on Venus formed by ejecta deposited above the atmosphere in an initially circularly symmetrical pattern, then winnowed eastward by zonal winds. The inner region is bright due to ejecta particles that are large compared with the radar wavelength. The dark parabola is poorly radar-backscattering, requiring a thickness of several cm of fine ejecta. Note the fairly sharp boundary between ejecta deposits darker than and brighter than the underlying terrain. The source is the crater Adivar at the center ($8.93 \pm N$, $76.22 \pm E$, 3 km across). Magellan image F-MIDR-10N076. Black stripe is missing data. Arrow indicates a “jet” flaring wider to the left that may be associated with the incoming bolide “vacuum tunnel.”

review). If the vacuum tunnel in the wave of the bolide is equal to the diameter of the crater (e.g., 10 km), it would take ~ 10 –50 sec to close at the speed of sound. In other words, the impact plume bursts out through the tunnel and into space, launching impact vapor and fine ejecta onto ballistic trajectories.

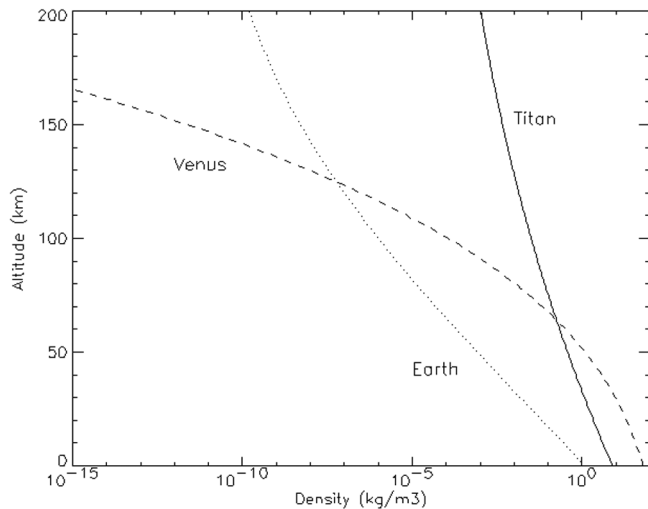


Fig. 3. Atmospheric density structure of Earth, Venus, and Titan. Low gravity and stratospheric heating by haze give Titan a large scale height, so its density falls off very slowly. Ejecta particles of 1 mm to 10 cm traverse their own mass of atmosphere over ~ 100 km distances (i.e., become appreciably affected by drag on the landform length scales under discussion in this study) when the density is 10^{-5} to 10^{-3} kg m^{-3} . Thus, ballistic or near-ballistic trajectories can occur on Earth and Venus above altitudes of ~ 40 – 110 km, but do not occur on Titan until altitudes of 200–500 km.

In contrast, on Titan, the tunnel to reach space vacuum (or at least low densities as described above) is around five times longer than on Venus and Earth. Impact velocities at Titan (see discussion in Lorenz [1997]) may typically be 3–10 km/s for saturnian impactors and Uranus-Neptune family comets, or exceptionally 20 km/s for the Oort Cloud comets. Thus, the 200–500 km plume expansion will occur at ~ 2 – 10 km/s, or will take 20–250 sec. The sound speed in Titan's atmosphere is 200–300 m/s, and a 10 km-wide tunnel will close in about 30–50 sec, the lower end of this range.

To recap, impact plume expansion on Titan is qualitatively different from that on Venus and Earth. On Titan, the bolide wake closes on a timescale comparable with or smaller than the time for the impact plume to expand along it, and, thus, ejecta is trapped within the atmosphere. On Venus and Earth, the energetic plume expands rapidly and the tunnel is short and, thus, the plume can readily burst into space to launch ejecta ballistically on timescales around an order of magnitude shorter than those needed for the wake to close off.

Hence, I direct attention to the material collimated by the plume in Titan impacts. As for radar observations of Venus, ejecta on Titan will form bright and dark features around craters, depending on the particle size. Unlike Venus, however, the trajectories of ejecta within the atmosphere do not begin with a circularly-symmetric deposition on top of the atmosphere, but in a linear cloud starting at the impact site and projecting along the bolide wake.

MODEL AND RESULTS

For predictive convenience (the streak morphologies are not strongly sensitive to the wind profile), I assume the zonal wind speed is a function of altitude h only, with $u(h) = h/2$ where u is in m/s and h in km—this simple expression agrees fairly well with the zonal wind model used for the Huygens probe mission design (e.g., Flasar et al. 1997). I have assumed that Titan's winds run prograde (W-E), as indicated by infrared spectroscopy (Kostiuk et al. 2001). Atmospheric density varies as $\rho(h) = \rho_0 \exp(-h/H)$ with H being the tropospheric scale height of ~ 20 km (the scale height in the stratosphere rises to >60 km). In the near-surface atmosphere, the terminal velocity V of ejecta particles (which are assumed not to interact with each other) is given as a function of their radius (r) as simply $V = 2*(r/0.01)^{0.5}$ (SI units) and varies as the inverse square root of $\rho(h)$. A more elaborate formulation would assign somewhat slower speeds for fine dust particles, but is not significant here. Vervack and Melosh (1992) describe implications of the terminal velocity function further.

The ejecta size distribution is assumed to be one where equal volumes (equivalently, masses) of ejecta are in each logarithmic size bin. The size distribution, assumed to run from 100 microns to 10 m diameter, is comparable with previous work by Schaller and Melosh (1998) and Vervack and Melosh (1992). Particles smaller than 100 microns are easily blown over distances so large that the thickness of the layer of these particles becomes invisibly small (and such particles are easily saltated away after the formation of the feature). Particles much larger than 10 m are substantially unaffected by the atmosphere and might be individually resolved by Cassini observations as individual ejecta blocks rather than part of a layer. Nominally, the ejecta is deposited at rest in a cylinder with a radius equal to that of the crater. Deviation from any of these assumptions will lead to modest changes in morphology of the formed streaks, but a refinement of any of them would require comparable refinement of all other assumptions, which is deferred until observations become available.

The downwind drift distance (Z) is calculated as a function of particle size and drop altitude by following the fall time and wind displacement in 1 km altitude steps. A thickness, scaled so that the total ejecta volume agrees with the expression above, of ejecta for each particle size bin is deposited in each cell of a grid of 1×1 km squares that lies within a circle of one crater radius, centered on a point Z eastward from the center of the tunnel at that altitude. Thus, the ejecta pattern is, geometrically, the superposition of filled circles downwind of the crater that are displaced from the crater by wind and the initial displacement along the bolide tunnel.

Two observable fields are computed. The first is the total ejecta thickness. This is calculated by scaling the calculated superposition of layers per cell by the total distal

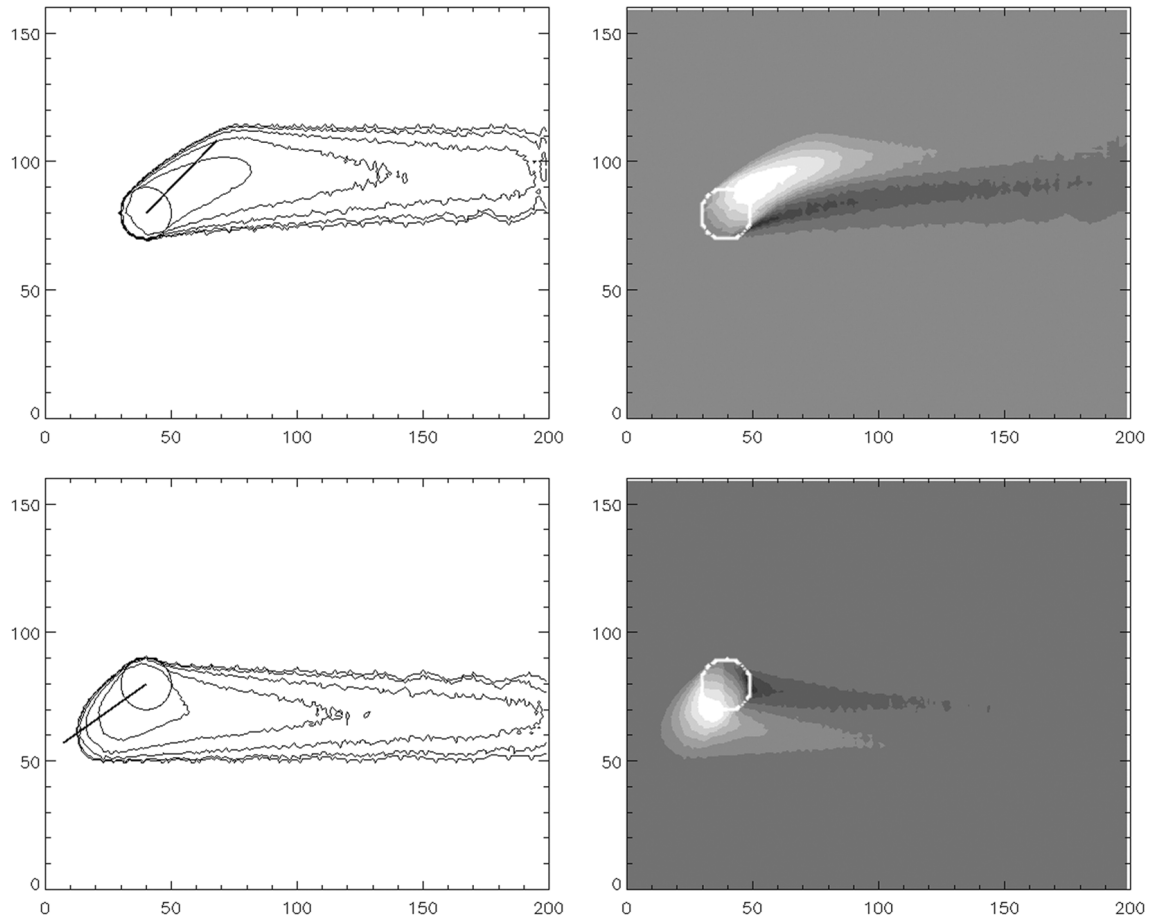


Fig. 4. Predicted ejecta thickness (left) and qualitative radar backscatter fields (right). The axes are in km. The thickness contours are 6, 2, 0.6, 0.2, and 0.06 m. The circle denotes a 20 km-diameter source crater. Ejecta is deposited in a cylinder 50 km long around the bolide trajectory with an incidence angle of 45° and an azimuth, indicated by the bold straight line, of 45° (top) and 235° (bottom). The backscatter grey scale is arbitrary.

ejecta volume divided by the total number of cells deposited. The distal ejecta volume is calculated based on the radar-visible extent of venusian parabolae, following Lorenz (2000) as $V = 7 \times 10^{-3} R_c^{3.27}$. This relationship, where R_c is the final crater radius (km) and V the ejecta volume in km^3 also agrees very well with the volume of microtektites launched from the few large impacts on Earth where the deposits are preserved. The contours of total ejecta thickness form a simple streak, smeared somewhat by the initial bolide tunnel footprint.

The second field, although calculated without an absolute scale, is more interesting. It is a predicted roughness, which will be observable as the radar cross section or reflectivity by the Cassini radar instrument (Elachi et al. Forthcoming). This instrument will map around 20% of the surface at high resolution (0.3–1 km) using synthetic aperture radar (SAR) techniques, and substantially more of the surface at a resolution of 50–100 km or better via scatterometry. Roughness may also be detectable as a signature in the microwave emissivity, although this may be

less prominent, and, in any case, will not be observed at high resolution. Ejecta particles larger than the radar wavelength (2.2 cm) are assumed to cause rough, radar-bright surfaces, while fine ejecta will make the surface smooth and, thus, radar-dark. These terms are of course only relative ones, since both surfaces may be radar-bright compared to, for example, hydrocarbon lakes. Even considering that the particles themselves may be somewhat radar transparent, there should be an observable distinction between ejecta-free surfaces and those covered by fine and coarse ejecta, respectively.

This distinction between bright and dark leads to a striking difference in appearance between the ejecta thickness and the radar cross section. The latter is divided into a long dark tail (the fine ejecta being carried further by wind) and a closer bright tail (one is reminded in some instances of the ion and dust tails of a comet, swept by the charged solar wind and by solar radiation pressure, respectively). Note that this dual-tail bright-dark morphology depends on the particle size to wavelength ratio peculiar to

radar and the process described here. The optical remote sensing instruments such as the visual and infrared mapping spectrometer (VIMS; Brown et al. Forthcoming) will, instead, sense primarily the optical “color” of the ejecta material itself, which presumably does not have a strong variation with particle size.

DISCUSSION

The computed fields are presented in Fig. 4. The observed morphology depends on the orientation of the incoming bolide with respect to the wind direction. If directly E-W or W-E, the ejecta thickness is largest since there is no latitude spread introduced. However, the dark and bright streaks are essentially superposed, and the net result is a rather weak streak of varying radar-brightness.

More generally, with an arbitrary bolide azimuth, the ejecta is spread out, while ejecta released at higher altitudes is deposited more north or south of the crater. The fine material drifts further, producing a dark streak strongly canted towards the east. The coarse, bright material drifts less, and for those bolide azimuths between 180 and 360°, the small drift at low altitudes is less than the displacement due to the release location to the west of the crater, so the bright material retains information on the incoming azimuth. Since the horizontal displacement of the release point is linearly related to the release altitude but drift increases as a stronger function of altitude (at least for the lowest part of the atmosphere, the part relevant here; more generally, the function is actually sigmoidal and flattens out after several scale heights), the drift exceeds the displacement and the ejecta is swept eastward. Thus, for westward azimuths, the bright streak has a “comma” shape.

The assumption that ejecta is deposited as a cylinder is probably the weakest of those employed in this simple study. However, the details of plume expansion and its interaction with the tunnel are not well-understood (e.g., Zahnle 1996), so no obvious alternative model presents itself. However, if the flared jet in Fig. 2 is associated with ejecta deposition from the tunnel, a deposition circle radius that increases with altitude might be a worthwhile starting point for future models.

CONCLUSIONS

A crater ejecta landform that may occur on Titan has been described. Ejecta plume expansion is qualitatively different on Titan and Venus due to the low impact velocity and plume expansion speed on Titan and its extended atmosphere. Distinct radar-dark and radar-bright “comet-tail” streaks form downwind of the source crater and are deposited within the atmosphere along the trajectory of the impacting bolide. The first radar images from Titan will be returned in October 2004. If, indeed, such features are found, variations

on the formation model described here (such as size distributions, deviations from cylindrical deposition, etc.) may be introduced to precisely fit the observed shapes, and thereby improve our understanding of the impact process and perhaps the wind profile on Titan.

Acknowledgments—This work was supported by the Cassini project. Comments by the referees led to an improved paper.

Editorial Handling—Dr. Anita Cochran

REFERENCES

- Brown R. H., Baines K. H., Bellucci G., Bibring J. P., Buratti B. J., Capaccioni F., Cerroni P., Clark R. N., Coradini A., Cruikshank D. P., Drossart P., Formisano V., Jaumann R., Langevin Y., Matson D. L., McCord T. B., Mennella V., Miller E., Nelson R. M., Nicholson P. D., Sicardy B., and Sotin C. Forthcoming. The visual and infrared mapping spectrometer. *Space Science Reviews*.
- Campbell D. B., Stacy N. J. S., Newman W. I., Arvidson R. E., Jones E. M., Musser G. S., Roper A. Y., and Schaller C. 1992. Magellan observations of extended impact crater related features on the surface of Venus. *Journal of Geophysical Research* 97:16249–16277.
- Crawford D. A. 1996. Models of fragment penetration and fireball evolution. In *The collision of comet Shoemaker-Levy 9 and Jupiter*, edited by Noll K. S., Weaver H. A., and Feldman P. D. Cambridge: Cambridge University Press. pp. 133–156.
- Elachi C., Allison M. D., Borgarelli L., Encrenaz P., Im E., Janssen M. A., Johnson W. T. K., Kirk R. L., Lorenz R. D., Lunine J. I., Muhleman D. O., Ostro S. J., Picardi G., Posa F., Rapley C. G., Roth L. E., Seu R., Soderblom L. A., Vetrilla S., Wall S. D., Wood C. A., and Zebker H. A. Forthcoming. RADAR: The Cassini Titan radar mapper. *Space Science Reviews*.
- Flasar F. M., Allison M. D., and Lunine J. I. 1997. Titan zonal wind model. In *Huygens: Science, payload, and mission*, edited by Wilson A. ESA SP-1177. Noordwijk: European Space Agency. pp. 287–298.
- Ivanov B. A., Basilevsky A. T., Neukum G. 1997. Atmospheric entry of large meteoroids: Implication to Titan. *Planetary and Space Science* 45:993–1007.
- Jessup K. L., Clarke J. T., Ballester G. E., and Hammel H. B. 2000. Ballistic reconstruction of HST observations of ejecta motion following Shoemaker-Levy-9 impacts into Jupiter. *Icarus* 146: 19–42.
- Kostiuk T., Fast K., Livengood T., Hewagama T., Goldstein J. J., Espenak F., and Buhl D. 2001. Direct measurement of winds on Titan. *Geophysical Research Letters* 28:2361–2364.
- Lorenz R. D. 1997. Impacts and cratering on Titan: A pre-Cassini view. *Planetary and Space Science* 45:1009–1019.
- Lorenz R. D. 2000. Microtektites on Mars: Texture and volume of distal impact ejecta deposits. *Icarus* 144:353–366.
- Lorenz R. D. and Hubbard W. B. 2001. Speed of sound in planetary atmospheres. In *Handbook of elastic properties of liquids, solids, and gases*. Volume 4, edited by Levy M., Bass H., and Stern R. San Diego: Academic Press.
- Lorenz R. D. and Mitton J. M. 2002. *Lifting Titan's veil*. Cambridge: Cambridge University Press.
- Melosh H. J. 1989. Impact cratering: A geologic process. Oxford University Press.
- Melosh H. J. and Vickery A. M. 1991. Melt droplet formation in energetic impact events. *Nature* 350:494–497.

- Schaller C. J. and Melosh H. J. 1998. Venusian ejecta parabolas: Comparing theory with observations. *Icarus* 131:123–137.
- Shultz P. H. 1992. Atmospheric effects on ejecta emplacement and crater formation on Venus from Magellan. *Journal of Geophysical Research* 97:16183–16248.
- Vervack R. J., Jr. and Melosh H. J. 1992. Wind interaction with falling ejecta: Origin of the parabolic features on Venus. *Geophysical Research Letters* 19:525–528.
- Walkden G., Parker J., and Kelley S. 2002. A late triassic impact ejecta layer in southwestern Britain. *Science* 298:2185–2188.
- Zahnle K. J. 1996. Dynamics and chemistry of SL9 plumes. In *The collision of comet Shoemaker-Levy 9 and Jupiter*, edited by Noll K. S., Weaver H. A., and Feldman P. D. Cambridge: Cambridge University Press. pp. 183–212.
-